

Dislocation-Cracks Interaction During Fatigue: A Discrete Dislocation Dynamics Simulation

I.N. Mastorakos and H.M. Zbib

In this article, the effect of different shape cracks on fatigue behavior in metals is investigated with the help of the discrete dislocation dynamics technique. The cracks are represented as distributions of infinitesimal dislocation loops. The distribution is determined by an integral equation satisfying stress-free boundary conditions and containing a singular kernel of the third type. The stress field in the cracked domain is calculated using a superposition principle coupled with an iterative technique. The derived stress fields describe the interaction between the cracks and the dislocations into the framework of dislocation dynamics. The simulation results provide an insight on the three-dimensional character of the dislocation structure around the cracks and its relation to the crack shapes. The effect of the cracks on the macroscopic yield stress is also determined for various crack sizes and shapes.

INTRODUCTION

The presence of cracks inside materials is critical for the fundamental understanding of materials behavior, especially under specific loading conditions like fatigue. Unlike brittle materials, ductile metals can fail in a fatigue test without any appreciable external stress. In general, small cracks that do not influence the strength of a ductile material diminish its fatigue strength. At the same time, the elastic fields associated with cracks lead to interactions with other defects (like dislocations) that influence fracture behavior, thereby affecting the strengthening mechanisms. In particular, dislocations in the vicinity of the crack tip play an important role in fracture. Many observations have shown that a dislocation

can either shield the crack, therefore preventing cracking, or open it further, thus enhancing the material susceptibility to failure. Furthermore, dislocation-free zones have been observed in

front of the crack tip, implying the absorption of dislocations by the crack surface. Therefore, the problem of crack dislocation interaction is fundamental to any model of crack tip plasticity, and different techniques to examine it are reported in the literature. For instance, using dislocation modeling, the stress field around an internal crack and the image force on a screw dislocation were obtained.¹

A dislocation emission criterion from a sharp crack tip by analyzing the ductile versus brittle behavior of crystals was also proposed.² An in-situ observation of the dislocation emission from a crack tip revealed the existence of a dislocation-free zone between crack tip and plastic zone,³ which led to the development of a dislocation-free zone model of fracture.⁴ In addition, the interactions of dislocations with various types of cracks were studied by using the conformal mapping technique, dislocation modeling method, and thermodynamic approach.

Recently, the screw dislocations around a radial surface crack in a circular bar⁵ and extended dislocations around a semi-infinite crack were investigated,⁶ and the effect of fatigue on the failure of irradiated materials has been studied for copper alloys and pure iron.^{7,8} Furthermore, discrete dislocation dynamics (DD) have been used to model the interaction between a sharp crack and dislocations.^{9,10} However, these approaches are two-dimensional (2-D) and do not consider complex loading conditions. Contrary to that approach, the approach presented here is three-dimensional (3-D).

In this article, cyclic loading conditions are considered to enable the study of the behavior of fractured materials under fatigue.

How would you...

...describe the overall significance of this paper?

This paper is an effort to study numerically the deformation of a material that contains multiple cracks with different shapes and sizes, under fatigue loading conditions. The yield stresses were found and compared with the uncracked material. The analysis shows that the cracked area size affects the yield stress, as well as the crack shape and stress field.

...describe this work to a materials science and engineering professional with no experience in your technical specialty?

The effect of different shaped cracks on fatigue behavior in metals is investigated. The cracks are represented as distributions of infinitesimal dislocation loops. The stress field of the cracks is calculated using a superposition principle. The simulation results provide an insight into the 3-D dislocation structure around the cracks and its relation to the crack shapes.

...describe this work to a layperson?

The presence of cracks inside materials changes their mechanical behavior. Since the plastic deformation of a material depends on the dislocation motion inside the material, and the dislocation motion is affected by the presence of the cracks, the investigation of the cracks-dislocation interaction is important when the deformation of a cracked material is considered. This paper tries to provide an insight into this matter.

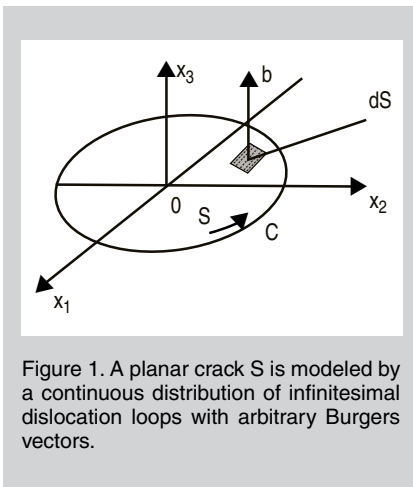


Figure 1. A planar crack S is modeled by a continuous distribution of infinitesimal dislocation loops with arbitrary Burgers vectors.

THE METHOD OF DISCRETE DISLOCATION DYNAMICS

In recent years 3-D DD have been developed to deal with nano- and microscale phenomena involving dislocations.¹¹ The simulated 3-D space is usually a cube with edges 3–30 μm that represents a single crystal. In DD, continuous dislocation lines or loops are approximated with sets of discrete straight-line segments. The self-stress of a single straight line dislocation for an infinite domain is known from the literature.¹² The sum of self-stresses of the discrete segments represents the overall self-stress of the curved dislocation lines. Knowing the self-stress, the interaction between dislocation segments can be calculated with the use of Peach–Koehler force (see Equation 1 in the Equations table) where \mathbf{b}_i represents the Burger vector and ξ_i the line sense of a dislocation segment i . The last term, $\mathbf{F}_{i\text{-self}}$, is the force due to the local interaction between the segment adjustment to nodes j and $j+1$. The total stress tensor σ_i^{total} at a given point is the sum of stresses from all dislocations, cracks, and any other internal and external agencies.

In 3-D dislocation dynamics all N dislocation nodes ($3N$ degrees of freedom) move simultaneously in the glide direction over a characteristic time corresponding to the time increment required for an interaction to take place. The result is a set of nonlinear differential equations governing the motion of the dislocation segments. The governing equation of glide motion for each dislocation node is a modification of Newton's second law as

shown in Equation 2, where m_i^* is the effective mass per unit dislocation, M is the mobility which depends on both temperature T and pressure p , \mathbf{v}_i is the glide velocity of segment i , and \mathbf{F}_i is the glide component of the Peach–Koehler force.¹³

CRACK REPRESENTATION USING A SUPERPOSITION PRINCIPLE

Two- and three-dimensional cracks can be represented with the use of a superposition principle. In two dimensions a distribution of edge and screw dislocations represents the crack, while in three dimensions infinitesimal dislocation loops are used instead.¹⁴ In this work, the superposition principle is used to represent 3-D cracks lying on a $z = z'$ plane. The crack area is considered to be a distribution of infinitesimal dislocation loops each with Burgers vector $\mathbf{b}(b_x, b_y, b_z)$ and infinitesimal area dS . A local Cartesian coordinate system $Oxyz$ is defined within each crack in order to describe the displacement field of the distribution (Figure 1).

The stress field of the distribution is obtained by differentiating its displacement field, applying Hooke's law, and considering only the stress components arising on plane $z = z'$ (since the crack plane is defined on the slip plane). The general form of these components is given in Equation 3, where $K_{ij}(\mathbf{x}, \mathbf{x}')$ is called the kernel of the distribution and physically represents the tractions induced on the slip plane due to an infinitesimal dislocation loop of unit strength. In general, a planar crack of any shape embedded in an infinite (or finite) body subjected to arbitrary loading will experience both opening and shearing mode displacements. Hence, one must assume a continuous distribution of infinitesimal dislocation loops, each of area dS and Burgers vector $\mathbf{b}(b_x, b_y, b_z)$, along the crack faces. The tractions on the crack plane induced by this distribution are obtained by integrating Equation 3 over the whole crack surface.

The superposition principle states that, in order to produce a traction-free surface, the above tractions must be equal and opposite to the total tractions $t_i^0(\mathbf{x})$ caused by both internal and ex-

Equations	
$\mathbf{F}_i = \sigma_i^{\text{total}} \cdot \mathbf{b}_i \times \xi_i + \mathbf{F}_{i\text{-self}}$	(1)
$m_i^* \frac{d\mathbf{v}_i}{dt} + \frac{1}{M_i(T,p)} \mathbf{v}_i = \mathbf{F}_i^{\text{glide-component}}$	(2)
$d\sigma_{3i}(\mathbf{x}) = K_{ij}(\mathbf{x}, \mathbf{x}') b_j(\mathbf{x}') dS$	(3)
$\iint K_{ij}(\mathbf{x}, \mathbf{x}') b_j(\mathbf{x}') dS = -t_i^0(\mathbf{x})$	(4)
$\iint K_{ij} b_j dS = b_i(x) \iint K_{ij} dS$ $+ b_{j,y}(x) \iint K_{nm}(-p_y) dS + \dots$	(5)
$\sum_{j=1}^N \sum_{m=1}^3 K_{ij}^{nmf_m} = t_i^0(x_j, y_j)$ ($i = 1, 2, \dots, N$)	(6)

ternal loads. The application of this superposition principle leads to the integral Equation 4.

The kernel $K_{ij}(\mathbf{x}, \mathbf{x}')$ introduces a third degree singularity to the integral Equation 4. This type of singularity appears in all problems involving crack representation by dislocations regardless of the geometry concerned. Due to that, the integral must be interpreted in the so-called Hadamard finite-part sense.¹⁵ Numerous numerical techniques are reported in the literature to solve Equation 4. Most of them use either boundary elements formulation^{16,17} or semi-numerical methods.^{18,19} The semi-analytical processes are very fast, but can only deal with cracks of specific shapes¹⁹ and usually fail when the external traction is very complicated or changes very fast. The boundary element formulations are computationally

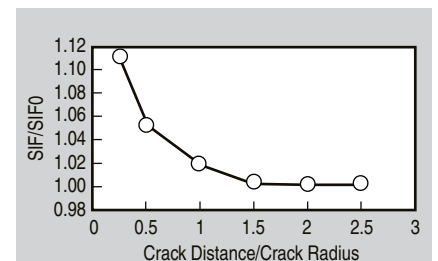


Figure 2. Normalized stress intensity factor (SIF) as a function of the normalized crack–crack distance. When the distance between cracks is more than ~ 2.5 crack radius, the SIF of each crack equals the SIF of the single crack.

slower, but are more general, allowing the consideration of random shape cracks, and they can deal with complicated tractions. Since the dislocation presence very close to the cracks will produce arbitrary tractions, the latter methods are more appropriate for this case.

The method used in this paper was first developed by Y. Murakami and S. Nemat-Nasser¹⁶ and later extended by D.N. Dai et al.¹⁷ Each component of Burger's vector \mathbf{b} (which in this case coincides with the unknown dislocation distribution) is expanded into a Taylor's series and by substituting it into integral 4, yielding Equation 5.

The resulting integrals on the right hand side of Equation 5 are weakly singular and can be derived using numerical techniques.¹⁷ The numerical solution is derived by dividing the crack plane into a number N of triangular elements. Within each element the unknown distribution b_j is assumed to be $b_j(x,y)=W(x,y)f_j$, where f_j is a constant to be estimated and $W(x,y)$ is a general shape function defined as $W(x,y)=\sqrt{2\alpha d(x,y)-d(x,y)^2}$. In this previous equation, α is a characteristic crack length and $d(x,y)$ is the distance of the center of each triangle from the crack face. The application of the above leads to Equation 6.

The solution of this system of equations provides the unknown constants f_j within each triangle. Then, the unknown distribution is evaluated directly by multiplying f_j with the shape function $W(x,y)$. Also, as shown by Hills, for the case of infinitesimal dislocation loops, the distribution function b_j represents the crack profile.¹⁴

In the case of two interactive cracks, an iterative procedure is used to calculate their stress field. According to this process, the first crack is calculated using the method described and considering only the external stress field. Then, the stress field of this crack is added to the external stress and the second crack is calculated. Next, the first crack is recalculated under the influence of the stress field of the second crack. The process is repeated until the crack face displacements of the two cracks converge.

After the crack opening displacements are found, the stress field pro-

duced by the cracks is calculated. These stresses will be used to simulate the interactions with dislocations through the DD framework. The validity of the method had been checked by calculating the crack opening displacement and the stress intensity factor (SIF) of a penny-shaped crack with 228 collocation points. The normalized SIF was found to be 0.6363, in very good agreement with the theoretical results of

0.6366.²⁰ Also, the image stresses were calculated for a penny-shape of 2,000b radius and the interaction with a dislocation in different positions above and below the crack has been investigated. The results showed the formation of shielding and amplification zones close to the crack area.²¹ These zones affect the crack shape, and therefore the behavior of the specimen under loading. Finally, the normalized SIFs of the two

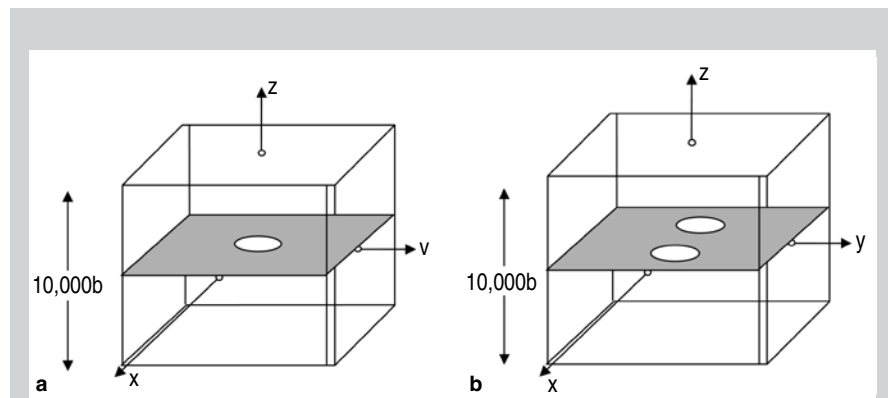


Figure 3. A schematic of the geometries used. The plane $z=0$ contained the cracks, and the dislocations produced by the F-R source (not shown) were moving on the (111) plane.

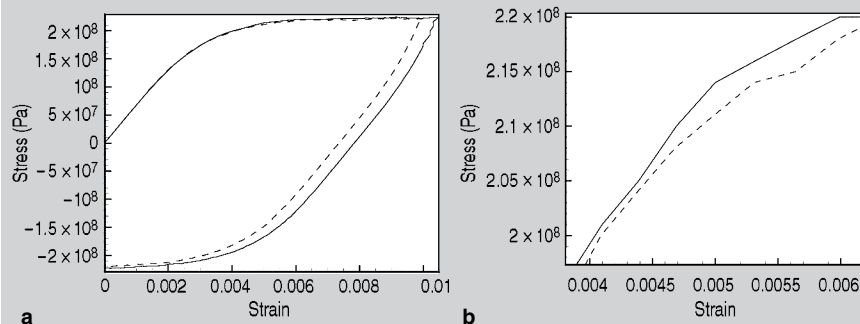


Figure 4. (a) Fatigue plots of two specimens, one without a crack and one containing a crack of radius 1,000b. Solid line: uncracked specimen; dashed line: cracked. (b) The difference between the yield stresses of the two specimens is very small but distinct.

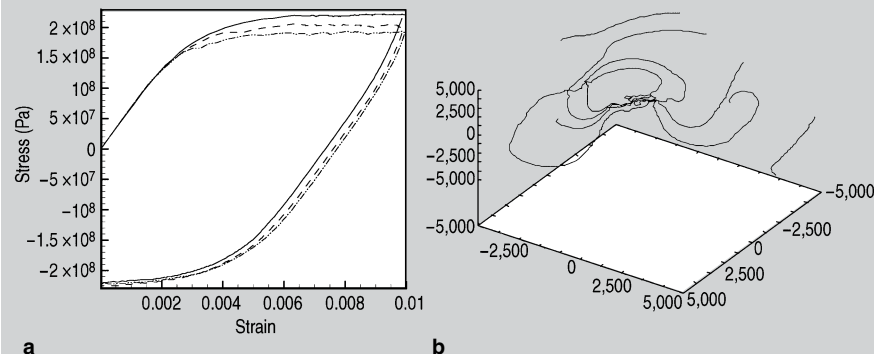


Figure 5. (a) Fatigue plots of three specimens containing a penny-shaped crack of different radius. Solid line: 1,000b; dashed line: 2,000b; dotted line: 2,500b. The behavior of the first specimen (1,000b crack radius) is closer to the uncracked specimen, as shown previously in Figure 2. (b) The dislocation structure in the second case when the strain was 0.01. The crack is situated in the middle of the specimen. The units of the axes are in Burgers vectors.

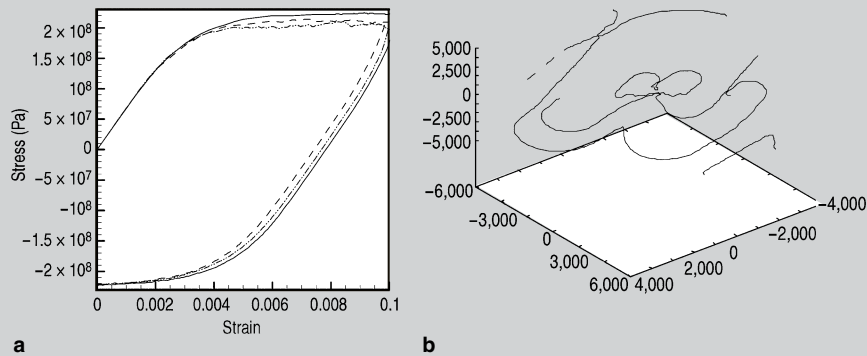


Figure 6. (a) Fatigue plots of three specimens containing elliptical cracks of different eccentricity (e). Solid line: $e=0.7$; dashed line: $e=0.75$; dotted line: $e=0.85$. The behavior of the first specimen ($e=0.7$) is again closer to uncracked specimens. (b) The dislocation structure in the second case when the strain was 0.01. The crack is situated in the middle of the specimen. The units of the axes are in Burgers vectors b .

cracks as a function of the distance between them were found. The results are shown in Figure 2.

FATIGUE AND CRACK PROFILES

The computation domain was a cube of side length $10,000b$, with b being the magnitude of Burger's vector. The x , y , and z axes were parallel to $[100]$, $[010]$, and $[001]$ directions, respectively, of a face-centered cubic (fcc) crystal. The origin was fixed at the center of the cube. Two types of computational experiments were performed: a specimen with a crack in its center and a specimen with two cracks on the same plane but at different distances from its center. In all cases the cracks were lying on plane $z=0$. Figure 3 shows all of the cases.

In order to study the fatigue behavior, a Frank-Read (F-R) source was positioned into the cubic specimen and a strain rate of 100 s^{-1} was applied. Reflection boundary conditions were used to simulate an infinite space.¹¹ For the case of the simple crack, the F-R source was initially on the (111) plane at a distance of $333b$ below crack plane. For the case of two cracks, the F-R source was positioned at the center of the specimen. Initially, an uncracked specimen was loaded in tension until a strain of 0.01 was achieved and the stress-strain curve was obtained. Then the simulation stopped and an opposite strain rate of -100 s^{-1} was applied and the new stress-strain curve was combined with the previous one to produce a fatigue cycle. These results, obtained from the uncracked specimen, were used as a reference to be compared with the results obtained from the cracked specimens. Then cracks were introduced into the specimen. In all cases a simple loading cycle similar to the one described above was used, and the yield stress was calculated at an offset strain of 0.2%.

First the case of a specimen with a penny-shaped crack of radius $1,000b$ was studied. The obtained stress-strain curve was compared with the curve corresponding to an uncracked specimen. The results are shown in Figure 4a. A first observation is that the stress-strain curve of the cracked specimen is too close to that of the uncracked one.

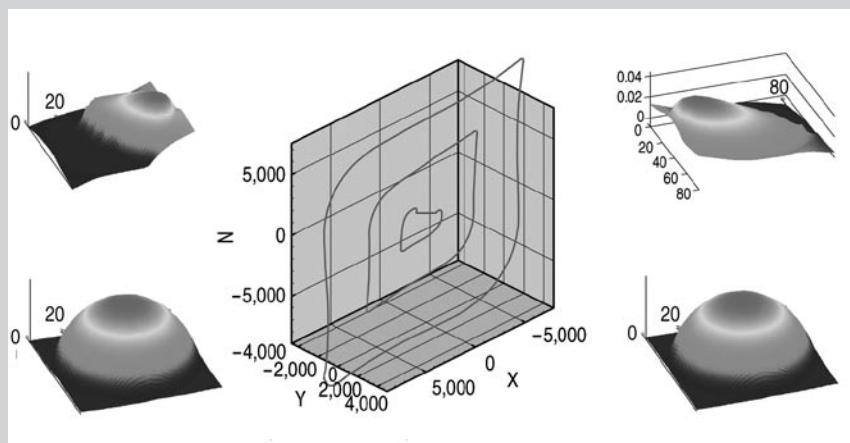


Figure 7. The dislocation structure for the case of two symmetric cracks. The middle distance is $7,000b$ and the initial F-R source is shown with the straight line in the middle of the specimen. The crack profiles correspond to the shearing crack displacement (along axis y), and the profiles below to the opening crack displacement (along axis z) for both cracks.

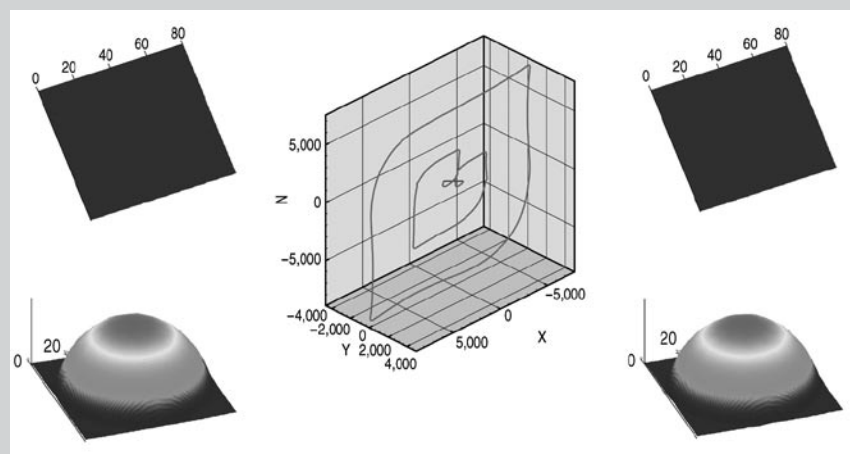


Figure 8. The dislocation structure for the case of two symmetrical cracks. The middle distance is $2,000b$ and the initial F-R source is shown with the straight line in the middle of the specimen. Notice that the source has produced fewer loops (compared to the previous case) due to the stronger stress field by the cracks. The crack profiles above, corresponding to the shearing crack displacement (along axis y), show a complete shielding along this direction. The profiles below correspond to the opening crack displacement (along axis z) again for both cracks.

However, the cracked specimen demonstrates a yield stress about 2% lower than the uncracked specimen. Another important feature is that the opposite loading leads to a stress-strain behavior similar to the uncracked specimen. This behavior can be explained by considering that the negative strain rate results in the crack closure, thus leading to the deformation of an uncracked specimen.

Two other cases were considered: one with a penny-shaped crack of radius 2,000b and one with a penny-shaped crack of radius 2,500b. The resulting stress-strain curves, together with the curve produced by the penny-shaped crack of radius 1,000b are shown in Figure 5a. Again, the results show a significant reduction of the yield stress of cracked specimens (~25% for the last case). Further, the specimen with the larger crack demonstrates the larger reduction of the yield stress. Finally, the dislocation structure associated with a total strain of 0.1% is shown in Figure 5b. The crack (not shown) is situated at the middle of the specimen, where the dislocation density is higher.

Similar results were produced by substituting the penny-shaped cracks with elliptical ones. Three cases were studied again: a crack with $a_1 = 2,000b$ and $a_2 = 1,400b$ (with a_1 and a_2 the axes of ellipse); a crack with $a_1 = 2,000b$ and $a_2 = 1,500b$; and a crack with $a_1 = 2,000b$ and $a_2 = 1,700b$. The obtained stress-strain curves are shown in Figure 5a. The above crack geometries result in elliptical cracks with eccentricity of $e = 0.7$, $e = 0.75$ and $e = 0.85$, respectively. Again, the dislocation structure associated with a total strain of 0.1% is shown in Figure 6b with the crack (not shown) at the middle of the specimen.

The results show a significant reduction of yield stress of cracked specimens. Like in the penny-shaped crack

case, the specimen with the larger crack (namely larger eccentricity) demonstrates the larger reduction of the yield stress.

Then, the two-crack case was studied. Three different cases were considered, all involving two penny-shaped cracks of radius 2,000b at different distances from each other. In this case, the specimen with cracks with the smallest distance showed the lowest yield stress. The reason is as the distance of the cracks is decreasing, the two cracks start behaving more like one crack of combined area. Previous studies have shown that the yield stress is inversely proportional to the cracked area.²² Also in this case, the dislocation structure is symmetrical, since the whole configuration is symmetrical now. In Figures 7 and 8 the dislocation configuration together with the crack profiles are shown for two different crack distances, namely 2,000b and 7,000b, respectively.

CONCLUSIONS

When fatigue experiments on a crystal containing cracks of different shapes and sizes were performed using DD, attention was focused on the continuous forward and reverse loading, the associated yield stress, and the crack profiles during the loading. It was found that the presence of a crack decreases the yield stress of the material. Also, the dislocations shield the cracks along some directions during the loading due to the symmetry of the configuration. The above seems to be valid only under tension. When the specimen is loaded under compression, the crack closes and the specimen's behavior in all cases approaches the behavior of the uncracked specimen. Nevertheless, it is possible that the dislocation structure can result in lower yield stresses under compression than the one obtained here

where no cross-slip was allowed. This case is currently under investigation and will be presented in an upcoming paper.

ACKNOWLEDGEMENT

The U.S. Department of Energy support under grant number DE-FG02-07ER4635 is gratefully acknowledged.

References

1. N.P. Louat, *Proc. 1st International Conference on Fracture*, 117 (1965), pp. 117-132.
2. J.R. Rice and R. Thomson, *Phil. Mag.*, 29 (1974), p. 579.
3. S.M. Ohr, *Mater. Sci. Eng.*, 72 (1985), p. 1.
4. S.J. Chang and S.M. Ohr, *J. Appl. Phys.*, 52 (1981), p. 7174.
5. K.M. Lin and H.L. Chang, *Mater. Sci. Eng.*, A187 (1994), p. 139.
6. Y.Z. Chen and K.Y. Lee, *Comp. Meth. Appl. Mech. Engng.*, 190 (2001), p. 4019.
7. B.N. Singh et al., *J. Nuclear Mater.*, 295 (2001), p. 1.
8. B.N. Singh, A. Horsewell, and P. Toft, *J. Nuclear Mater.*, 271-272 (1999), p. 97.
9. V.S. Deshpande, A. Needleman, and E. Van der Giessen, *Acta Materialia*, 51 (2003), p. 1.
10. A. Needleman, *Acta Materialia*, 48 (2000), p. 105.
11. H.M. Zbib, M. Rhee, and J.P. Hirth, *Int. J. Mech. Sci.*, 40 (1998), p. 113.
12. J.P. Hirth and J. Lothe, *Theory of Dislocations* (New York: Wiley Publ. Company, 1982).
13. H.M. Zbib and T. Diaz de la Rubia, *Int. J. Plasticity*, 18 (2002), p. 1133.
14. D.A. Hills et al., *Solution of Crack Problems* (Dordrecht, The Netherlands: Kluwer Academic Publ., 1996).
15. J. Hadamard, *Lectures on Cauchy's Problem in Linear Partial Differential Equations* (New York: Dover Publ. Inc., 1953).
16. Y. Murakami and S. Nemat-Nasser, *Engng. Frac. Mech.*, 16 (1982), p. 373.
17. D.N. Dai, D. Nowell, and D.A. Hills, *J. Mech. Phys. Solids*, 41 (1993), p. 1003.
18. Y.Z. Chen and K.Y. Lee, *Comp. Meth. Appl. Mech. Engng.*, 190 (2001), p. 4019.
19. Q. Wang et al., *Int. J. Frac.*, 108 (2001), p. 119.
20. G.R. Irwin, *J. Appl. Mech.*, 29 (1962), p. 361.
21. I.N. Mastorakos and H.M. Zbib, "Shielding and Amplification of a Penny-Shape Crack Due to the Presence of Dislocations," *Int. J. of Fracture*, 142 (2006), p. 103.
22. I.N. Mastorakos and H.M. Zbib, "DD Simulations of Dislocation-Crack Interaction During Fatigue," *J. ASTM International*, 4 (8) (2007), p. 1.

I.N. Mastorakos and H.M. Zbib are with the School of Mechanical and Materials Engineering, Washington State University, Pullman, WA 99164-2920. Prof. Mastorakos can be reached at mastorakos@mail.wsu.edu.